Desalination and Water Treatment
www.deswater.com

doi: 10.5004/dwt.2020.26154

202 (2020) 38–47
October

Preparation and characterization of partially degradable hollow fiber membranes based on polysulfone/poly(L-lactide-co-glycolide-co-ε-caprolactone) blends

Cezary Wojciechowski[a,*], Magdalena Mazurek-Budzyńska[b], Anna Palinska[b], Andrzej Chwojnowski[a], Ludomira Granicka[a], Wioleta Sikorska[a], Gabriel Rokicki[b]

[a]*Nałęcz Institute of Biocybernetic and Biomedical Engineering PAS, Trojdena 4 str., 02-109 Warsaw, Poland, emails: cwojciechowski@ibib.waw.pl (C. Wojciechowski), achwoj@ibib.waw.pl (A. Chwojnowski), lgranicka@ibib.waw.pl (L. Granicka), wsikorska@ibib.waw.pl (W. Sikorska)*
[b]*Department of Chemistry, Warsaw University of Technology, Noakowskiego 3 str., 00664 Warsaw, Poland, emails: mmazurek@ch.pw.edu.pl (M. Mazurek-Budzyńska), ania_palinska@o2.pl (A. Palinska), gabro@ch.pw.edu.pl (G. Rokicki)*

Received 2 October 2019; Accepted 23 May 2020

ABSTRACT

The method of preparation of partly degradable asymmetric hollow fiber membranes based on polysulfone/poly(L-lactide-co-glycolide-co-ε-caprolactone) blends (PSf/LGC) is presented. The membrane-forming blends were prepared by mixing two solutions: PSf in *N*-methyl-2-pyrrolidone and LGC in tetrahydrofuran. Further, PSf/LGC membranes were obtained by a dry/wet-spinning phase-inversion technique and treated with a sodium hydroxide solution using the flowing method. The membrane properties such as hydraulic permeability coefficient (UFC), retention coefficients, and structure morphology were evaluated before and after hydrolysis. An increase in the ultrafiltration coefficient was observed, while the retention coefficient did not change significantly in the case of membranes after post-treatment. The hydrolysis of LGC component in the terpolymer was evaluated by the weight method. Measurements of membrane weight loss before and after the hydrolysis process confirmed the removal of more than 50 wt.% of the LGC component from investigated membranes, resulting in permeability increase due to increased membrane porosity. Fourier transform infrared spectroscopy (FTIR) analysis also confirms significant LGC polymer removal. Furthermore, a computer-aided image processing method was used for investigating the morphology before and after the hydrolysis process. This method verified the changes in membranes' morphology by the differences of membranes' porosity. The total porosity of membranes increased from 34% to 38% to 42% after the hydrolysis process.

Keywords: Hollow fiber membranes; Retention; Degradation; Hydrolysis; Fouling

1. Introduction

Polysulfone (PSf) membranes have many valuable advantages such as high chemical, thermal, and mechanical resistance as well as hydraulic stability, however, they have shown some disadvantages [1–6]. The most important being collecting organic compounds on the surface and in the inner structure of the membrane, which leads to the clogging of the membrane pores. This process is called fouling [7,8]. The fouling phenomenon is an inherent problem present among membranes applied in the biotechnological field. In biotechnological processes, the fouling phenomenon which occurs, often causes membrane flux and decline of selectivity resulting in a decrease in efficiency [9–12].

* Corresponding author.

Therefore, some modifications are often necessary in order to improve the flux efficiency of membranes.

There are many methods to eliminate or reduce a fouling effect [13–22]. The most common is to increase the hydrophilicity of the membranes through the addition of a hydrophilic compound to the membrane-forming solution, or to modify the membrane's surface [23–26]. For instance, the pore formers such as polyvinylpyrrolidones or poly (ethylene glycol)s increase hydrophilicity and the membrane's porosity [27,28]. In our previous studies, we described the methods for obtaining partially degradable blends of PSf/polyurethane [29] and PSf/cellulose acetate [30,31] membranes, the porosity of which increases over time by reduction of the fouling effect.

In this study, the method of reducing a fouling effect in PSf membranes is presented. We hypothesized that it is possible to effectively increase the membranes' lifetime during their operation and overcome the fouling process. Our aim was to develop the new PSf membrane, which – despite the long time bio-fouling – would maintain constant permeability with a fixed cut-off point. We investigated the possibility of obtaining a membrane using a mixture of hydrolytically stable and hydrolyzable polymers. In order to reduce the fouling effect, two-component membranes capable of partial degradation have been designed. One of the components would degrade during the process, whereas the porosity would increase, causing an increase in membranes' efficiency and their working time. The membrane was hypothesized to increase its hydraulic permeability in time. For this purpose, partial removal of one of the polymers from the membrane is necessary.

The basic membrane component was PSf, while the second component – poly(L-lactide-co-glycolide-co-ε-caprolactone (LGC) terpolymer – was removed from the membranes by a hydrolysis process [32]. This was possible because the LGC contained has ester groups in its structure, which decompose in the hydrolysis process. It is worth to note, that the changes of the membrane's structure after hydrolysis do not weaken the membrane's strength. The LGC in the PSf/LGC mixed membrane acts as a kind of porophore, with the difference that classic porophores flush quickly from the membrane, while LGC flushes slowly depending on the environment in which the membranes are applied. It can be alkaline, acidic, neutral, or it can contain enzymes. In aqueous solutions in which membranes are used, the slow hydrolysis of ester groups contained in LGC will occur, leading to the disintegration of this polymer and washing out of the membrane. In this way, the membrane structure will become more and more loose. This will lead to an increase in the penetration flow through the membrane medium. At the same time, progressive fouling during the operation of the membranes will reduce the flow and efficiency of the process. Therefore, a gradual increase in the porosity of membranes should limit fouling and allow a longer time of their application, which is the purpose of our modification.

2. Experimental

2.1. Materials

Polysulfone (PSf) (Udel 1,700 NT LCD from Dow Corning, M_w = 70,000 g mol^{-1}) LGC (molar ratio LA/GL/CL was 72:12:16, M_w = 78,400 g mol^{-1}, produced in centre of polymer and carbon material PAS, Zabrze, Poland [33], *N*-methyl-2-pyrrolidone (NMP) (Sigma Aldrich), tetrahydrofuran (THF) (Merck, Germany), polyethylene glycols (PEG) (Fluka, Germany, M_w = 4,000; 15,000; and 35,000 g mol^{-1}), chicken egg albumin (CEA) (Fluka, Germany, M_w = 45,000 g mol^{-1}), bovine serum albumin (BSA) (Fluka, Germany, M_w = 67,000 g mol^{-1}), sodium hydroxide (POCH). Glycerin (POCH) was dried overnight under vacuum at 100°C before usage. NMP was used as the solvent for PSf. THF was used as the solvent for LGC. NMP and THF were dried with a molecular sieves 4A (POCH) before usage.

2.2. Hollow fiber membranes fabrication

Polysulfone (PSf) and LGC were selected as the material for the blending of hollow fiber membrane fabrication. The PSf with NMP and LGC with THF were stirred at 20°C until complete dissolution. After that, both polymer's solutions were mixed together. The PSf/LGC weight ratios were 9/1, 8/2, 7/3, 6/4, and 5/5. Concentration of the polymer mixtures (PSf and LGC together) in NMP-THF solutions was constant and equal to 20 wt.%. The PSf and LGC polymers creates a blend, therefore, it is possible to selectively remove the LGC from the membrane structure.

The membranes were obtained by a dry/wet-spinning, using the plant constructed in Nałęcz Institute of Biocybernetic and Biomedical Engineering PAS (IBIB), by phase-inversion technique through extrusion of polymer solution.

The hollow fiber membrane were prepared by inserting twenty (6 cm long) pieces of hollow fiber into a polypropylene module (surface area about 25 cm^2). Both ends of the modules were sealed with an epoxy resin. Five types of PSf/LGC membranes with different PSf/LGC weight ratio were produced, marked as PSf/LCG 9/1, PSf/LCG 8/2, PSf/LCG 7/3, PSf/LCG 6/4, and PSf/LCG 5/5.

2.3. Membrane hydrolysis

The PSf/LCG membranes were treated with a 1 M NaOH water solution using the flowing method. Briefly, 1 dm^3 NaOH solution was passed through the membrane module passing inside the hollow fibres and flowing through the hollow fiber walls to the outside of module at 100 hPa transmembrane pressure. The hydrolysis process was held at the 20°C. After membrane hydrolysis was finished, pure water was flushed in both directions through the membrane walls in order to remove residual sodium hydroxide and products of hydrolysis decomposition.

The methods applied for evaluation of the membrane physical features like permeability, retention coefficient, morphology (using scanning electron microscopy (SEM) analysis) were described in our previous articles [29,30].

2.4. Comparative evaluation of porosity in membranes subjected to hydrolysis

MeMoExplorer is an original computer system designed for automation of the procedures of analysis of membrane section images. It makes it possible to analyze single as well

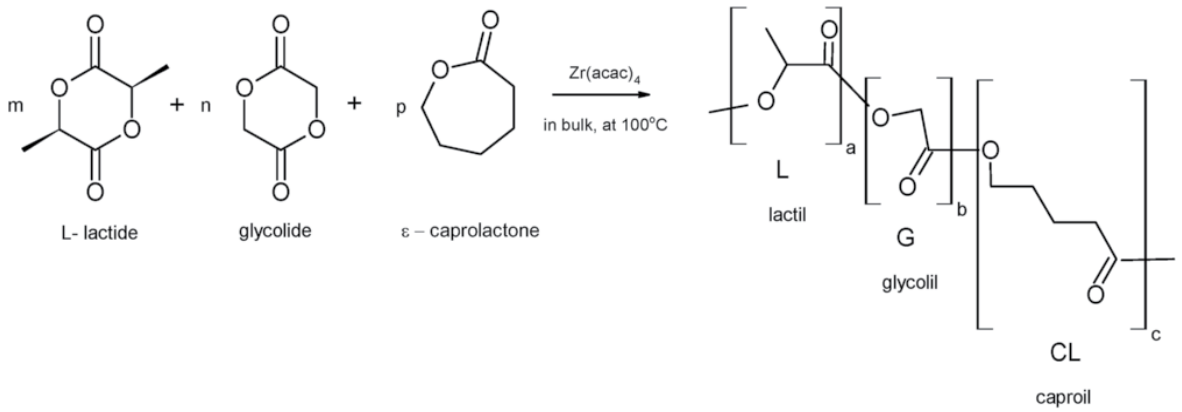

Fig. 1. Synthesis of poly(L-lactide-co-glycolide-co-ε-caprolactone) (LGC).

as serial images. In particular, image preprocessing and evaluation of morphometrical parameters used for the quality assessment of membranes can be performed. The system is logically coherent and can be used together with other software tools like Microsoft Excel. In our case, the preliminary operations have been performed by the MeMoExplorer [34] procedures chosen for a given problem.

2.5. Fourier transform infrared spectroscopy analysis

LGC defect size of PSf/LGC membrane was assessed by Fourier transform infrared spectroscopy (FTIR) analysis. The samples were powdered in liquid nitrogen Dried samples were placed on the crystal and pressed to it with the strength of 2 kg. IR spectra were recorded on a Varian Excalibur (US-California) FTIR spectrometer over attenuated total reflectance element with diamond crystal.

3. Results and discussion

3.1. Membranes weight loss measurements

In order to investigate the extent of the NaOH-based hydrolysis of the material, the membranes' weight loss was evaluated before and after hydrolysis process. The amount of LGC in membrane module was between 10 and 50 wt.% (PSf/LGC 9/1%–10%, PSf/LGC 8/2%–20%, PSf/LGC 7/3%–30%, PSf/LGC 6/4%–40%, and PSf/LGC 5/5%–50%). The measurements were repeated twice for each PSf/LGC composition. The results of LGC weight change are as shown in Table 1.

Differences in LGC weight loss in all types of membranes were comparable to each other and ranged from 56 to 75 wt.%. These results indicate that the LGC was effectively removed from the membrane structure acting as a typical pore former and has considerable influence on membrane structure as well as membrane flux.

3.2. Scanning electron microscopy of membranes

The PSf/LGC membranes cross-sections before and after hydrolysis are presented in Figs. 2–6.

Over a 50 wt.% of LGC removal from all types of PSf/LGC membranes causes new inner canal openings inside the membrane structure. After the removal of the LGC, the created structure is more dispersed and porous. These changes in the structure are the most probable reason for the increase in membrane permeability.

3.3. Membranes hydraulic permeability

The hydraulic permeability of membranes was measured (method is described in reference 30) before and after the NaOH-based hydrolysis. The observed values are shown in Table 2.

The PSf/LGC membranes coefficients of hydraulic permeability (UFC) before hydrolysis increased from 0.15 $cm^3\ min^{-1}\ m^{-2}\ hPa^{-1}$ for PSf/LGC 9/1 membrane to 3.7 $cm^3\ min^{-1}\ m^{-2}\ hPa^{-1}$ for PSf/LGC 5/5 membrane. Similarly, UFC of membranes after hydrolysis increased from 1.6 $cm^3\ min^{-1}\ m^{-2}\ hPa^{-1}$ for PSf/LGC 9/1 membrane

Table 1
Measurements of membranes mass before and after hydrolysis

Membrane	Membrane weight before hydrolysis (g)	LGC weight before hydrolysis (g)	LGC weight loss after hydrolysis (g)	LGC weight loss after hydrolysis (%)
PSf/LGC 9/1	0.12997	0.01300	0.00960	74
PSf/LGC 8/2	0.06929	0.01386	0.00780	56
PSf/LGC 7/3	0.09965	0.02989	0.01655	55
PSf/LGC 6/4	0.09335	0.03734	0.02800	75
PSf/LGC 5/5	0.11300	0.05650	0.03670	65

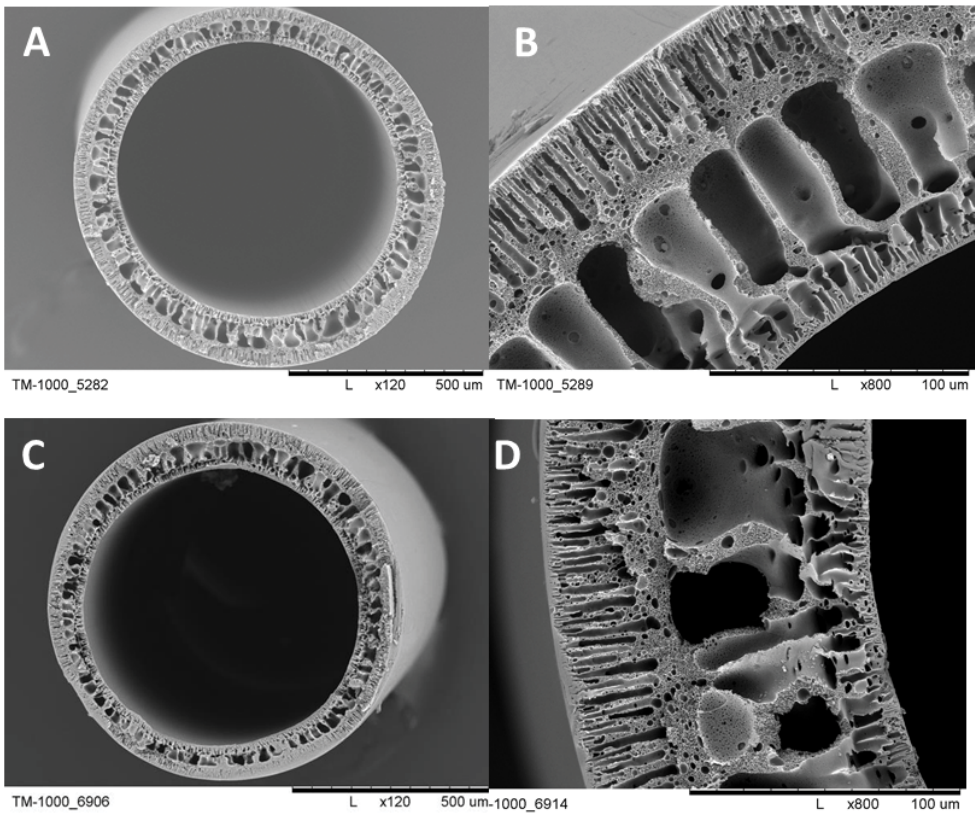

Fig. 2. Cross-section PSf/LGC 9/1 membrane before the hydrolysis (A and B), and after the process of the hydrolysis (C and D).

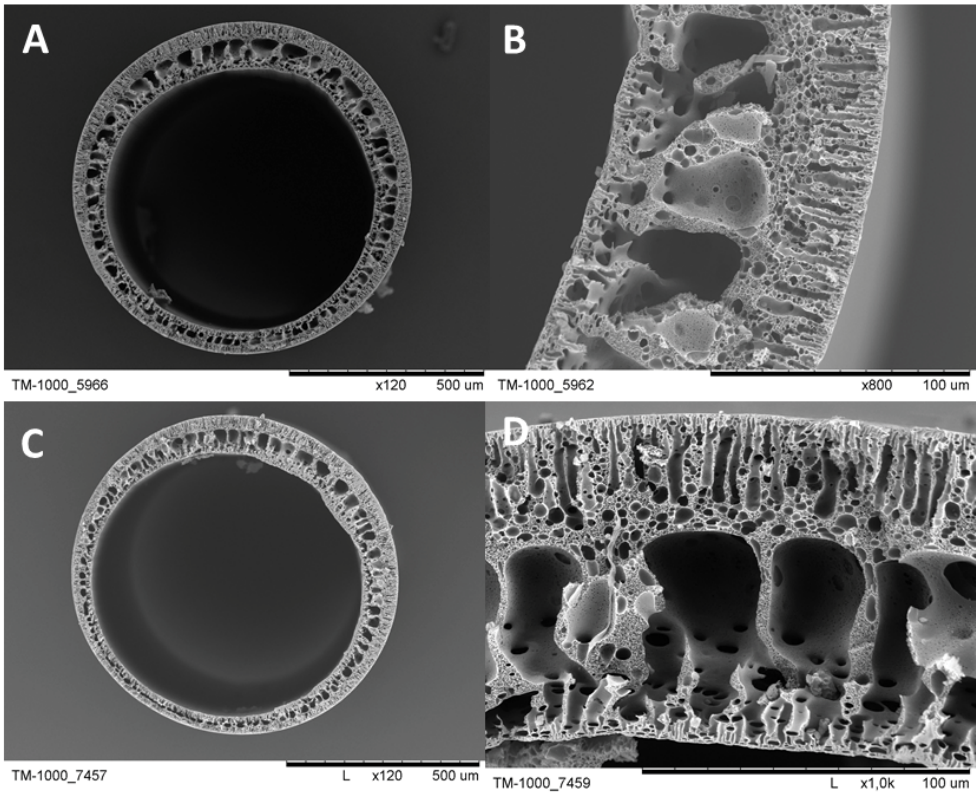

Fig. 3. Cross-section PSf/LGC 8/2 membrane before the hydrolysis (A and B), and after the process of the hydrolysis (C and D).

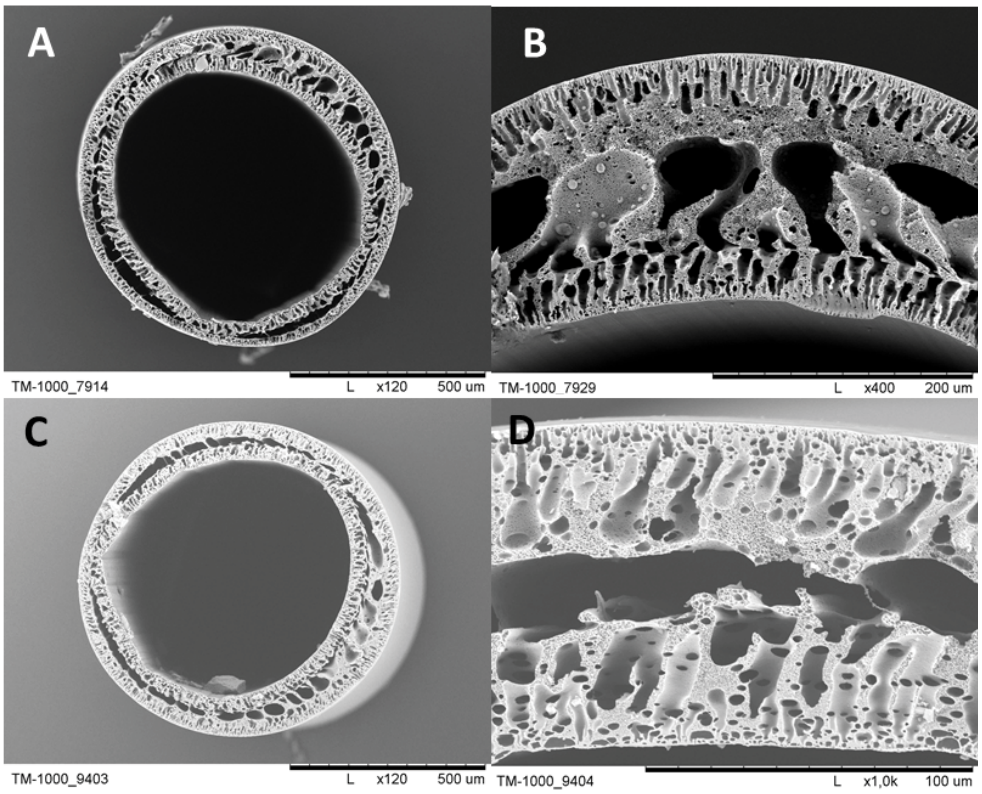

Fig. 4. Cross-section PSf/LGC 7/3 membrane before hydrolysis (A and B), and after the process of hydrolysis (C and D).

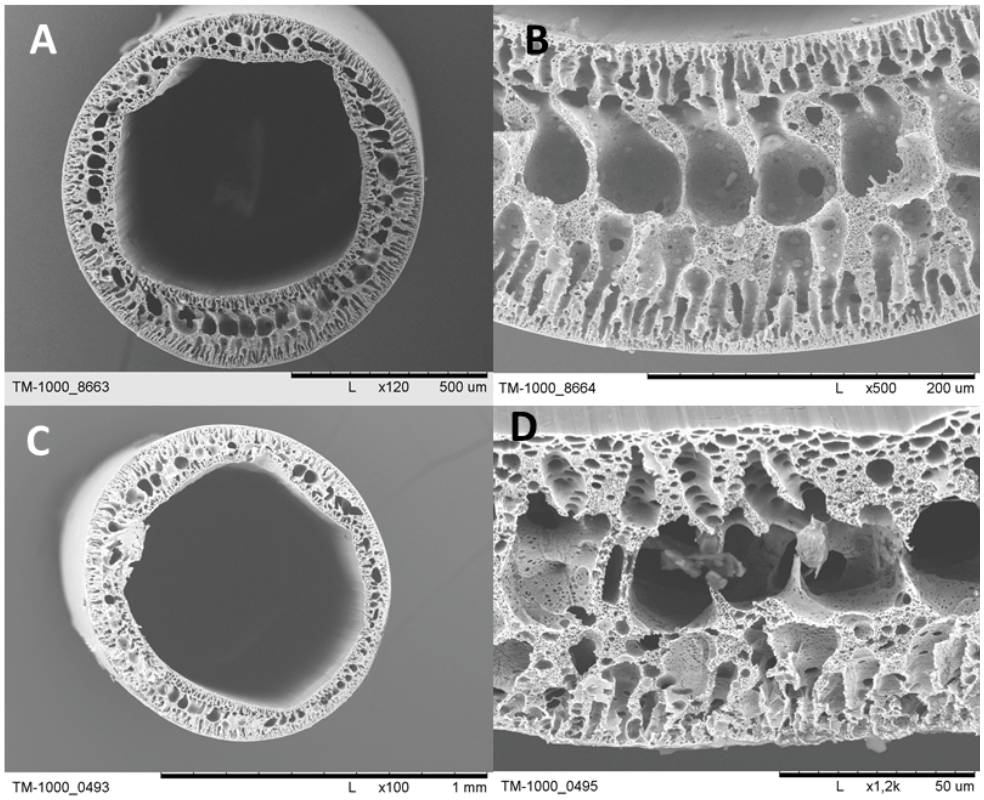

Fig. 5. Cross section PSf/LGC 6/4 membrane before hydrolysis (A and B), and after the process of hydrolysis (C and D).

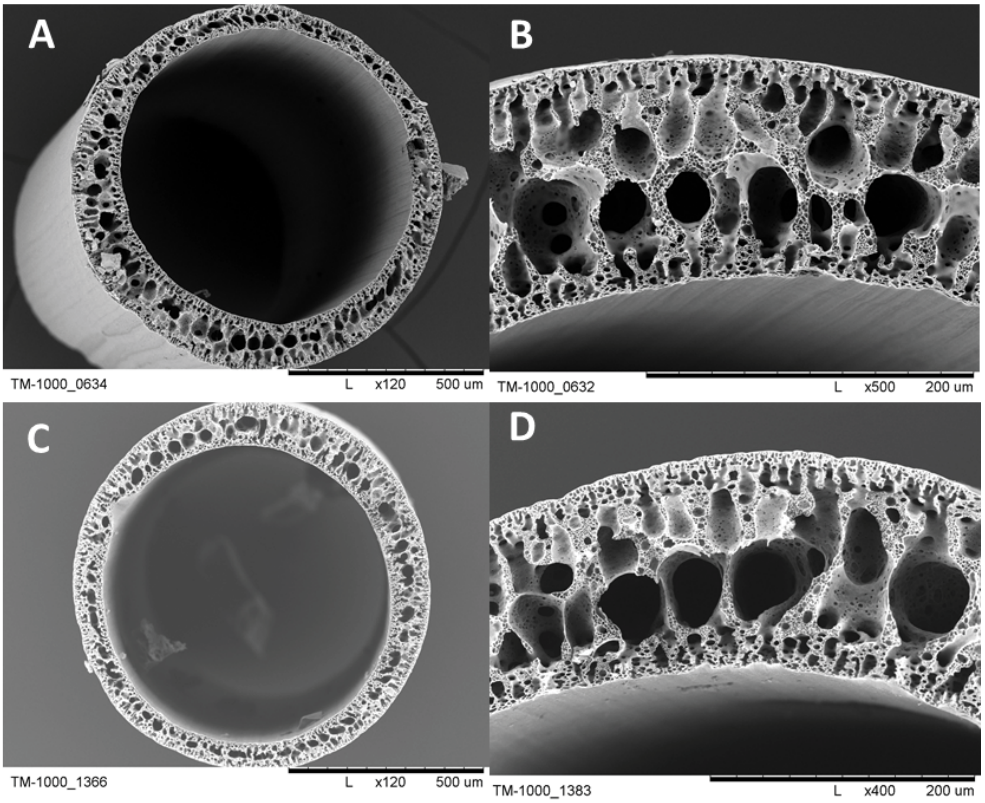

Fig. 6. Cross section PSf/LGC 5/5 membrane before hydrolysis (A and B), and after the process of hydrolysis (C and D).

Table 2
Coefficient of hydraulic permeability (UFC) for membranes before and after hydrolysis

Membrane	PSf/LGC 9/1	PSf/LGC 8/2	PSf/LGC 7/3	PSf/LGC 6/4	PSf/LGC 5/5
UFC before hydrolysis ($cm^3\ min^{-1}\ m^{-2}\ hPa^{-1}$)	0.15	0.2	2.4	3.3	3.7
UFC after hydrolysis ($cm^3\ min^{-1}\ m^{-2}\ hPa^{-1}$)	1.6	1.9	6.6	10.0	12.4
UFC after hydrolysis/UFC before hydrolysis	10.7	9	2.8	3	3.4

to 12.4 $cm^3\ min^{-1}\ m^{-2}\ hPa^{-1}$ for PSf/LGC 5/5 membrane. The LGC is more hydrophilic than the PSf, hence the increase of the LGC content in PSf/LGC membranes causes the permeability increase. The noticeable increase in the UFC after hydrolysis (from 2.8 to 10.7 times) was a result of the LGC partial removal from the membrane, which created the higher pores void volume of membrane (SEM picture, Figs. 2–6) facilitating the water flow.

3.4. Retention coefficients and molecular weight cut-off

The membrane retention coefficients before and after NaOH-based hydrolysis of markers: PEG 4,000; 15,000; and 35,000 g mol^{-1} as well as CEA 45,000 and BSA 67,000 g mol^{-1} were evaluated. Retention coefficient values for different markers of given molecular weights are shown in Fig. 7.

LGC polymer removal from the membrane led to the increase in membrane porosity and enhanced the membrane flux. Therefore, there are evident differences in retention values before and after membrane's hydrolysis. All retention values after hydrolysis were lower for the five types of the PSf/LGC blend membranes, compared to the retention values before hydrolysis. There were no changes observed in retention values for all types of membranes for 4,000 g mol^{-1} marker evaluation. Retention values for 15,000 and 35,000 g mol^{-1} markers were lower after hydrolysis in comparison to retention values before hydrolysis, especially for PSf/LGC 6/4 and 5/5 membranes with the largest LGC contents. Retention values for PSf/LGC 9/1, 8/2, and 6/4 membranes for 45,000 g mol^{-1} marker and for PSf/LGC 7/3 and 5/4 membranes for 67,000 g mol^{-1} marker were similar before and after hydrolysis in the amount of 90%. Hence 45,000 g mol^{-1} value is the molecular weight cut-off (MWCO) for PSf/LGC 9/1, 8/2, and 6/4 membranes and 67,000 g mol^{-1} values is the MWCO for PSf/LGC 7/3 and 5/5 membranes. It was observed that the hydrolysis did not influence the membrane cut-off value. As a consequence, hydrolysis did not change the evaluated membrane separation parameters. Although the membrane retention values for different markers changed, the membrane MWCO remained unchanged.

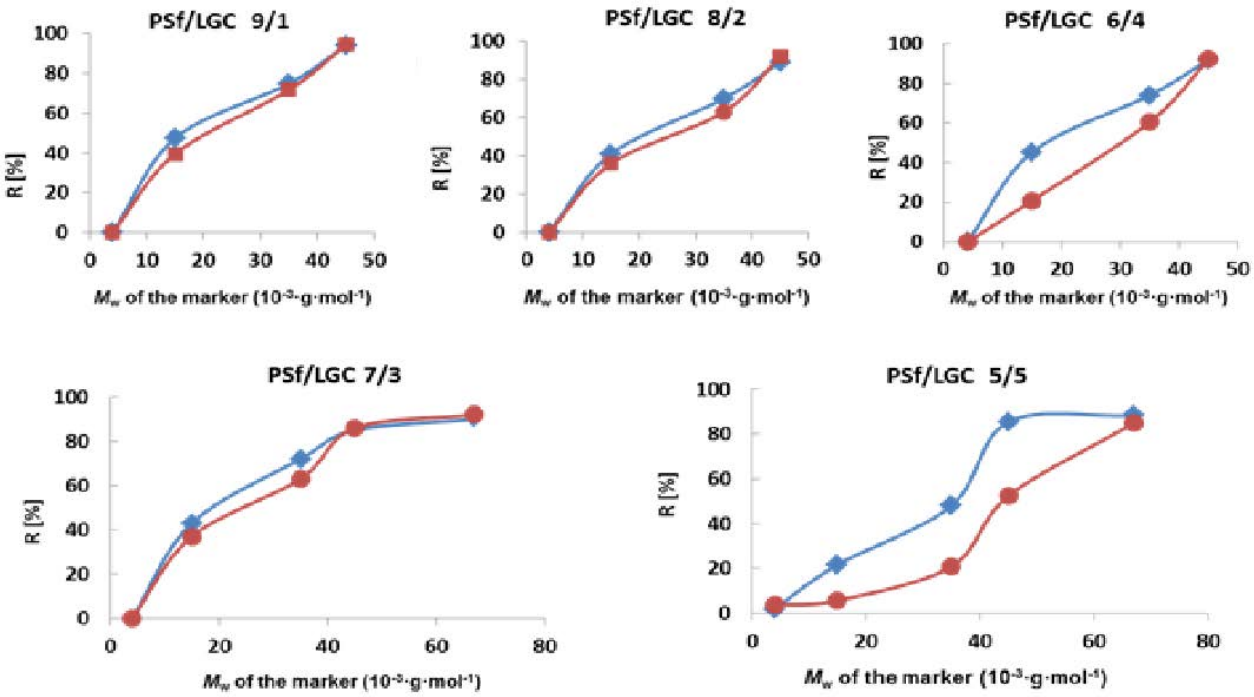

Fig. 7. Retention coefficient values for different markers obtained for membranes before and after hydrolysis. The values of curves before hydrolysis are marked as diamonds and after hydrolysis – as spheres.

The significant loss of membrane weight after removal of over a half of LGC polymer causes large macropores to appear and increased the porosity in the membrane structure. In conclusion, the LGC removal from membranes reduced retention parameters and allowed larger molecules to pass.

3.5. Comparative evaluation of porosity in membranes subjected to hydrolysis

The basic morphological parameters such as the porosity and size of pores of the membranes were tested by a computer analysis of SEM images. For porosity tests, we selected two membranes: PSf/LGC 6–4 and PSf/LGC 7–3. For benchmarking, we selected 20 cross-section SEM images for each membrane under 1,000 times magnification. Figs. 8 and 9 presents porosity *P* [%] of membranes before and after hydrolysis. Both figures describe the porosity of the membranes by pore size, grouped in fixed size-ranges: 0–3, 3–8, 8–20, 20–80, 80–100, 100–150, 150–300, and >300 μm², in relation to the total image surface. The last graph in both figures shows the total porosity in relation to the total cross-sectional area of the membrane.

The differences between pores' sizes before and after hydrolysis are visible, especially for pores of more than 300 μm in size. The number of pores over 300 μm in size increased from 5% to 20% for a PSf/LGC 6–4 membrane and from 2.5% to 17% for PSf/LGC 7–3 membrane after hydrolysis process. Moreover, the total porosity of membranes increased after hydrolysis from 34% to 42% for PSf/LGC 6–4 membrane and from 38% to 42% for PSf/LGC 7–3 membrane. This allows us to conclude that the hydrolysis process had an influence on morphological parameters of the membrane. Membranes after hydrolysis are much looser, which leads to a greater flow.

3.6. FTIR analysis

For FTIR measurements, a Psf/LGC 7/3 membrane was selected. Fig. 10 shows the spectrum of the membrane before hydrolysis (in green) and after hydrolysis (in blue). The 1,765 cm^{-1} peak corresponds to the C=0 carbonyl group contained in the LGC polymer's ester groups. The peak corresponding to the carbonyl group in Fig. 10. A is smaller by approximately 60% after hydrolysis, which proves removal of LGC polymer from the membrane.

4. Summary

The purpose of this work was to obtain partially degradable asymmetric PSf/LGC blend hollow fiber membranes of specific properties. In the process of inversion phases, five types of the PSf/LGC membranes of different composition have been obtained. The LGC polymer contents in PSf/LGC membrane were 10, 20, 30, 40, and 50 wt.%, respectively. The applied LGC polymer contained degradable ester groups. All types of PSf/LGC membranes were treated with 1 M NaOH water solution using the flowing method. The LGC degradation processes that consisted of hydrolysis caused the partial cleavage of ester bonds and disintegrated into low molecular oligomers and mers, which were washed out with water from the structure of membranes. Membranes mass measurements before and after the process of hydrolysis confirm

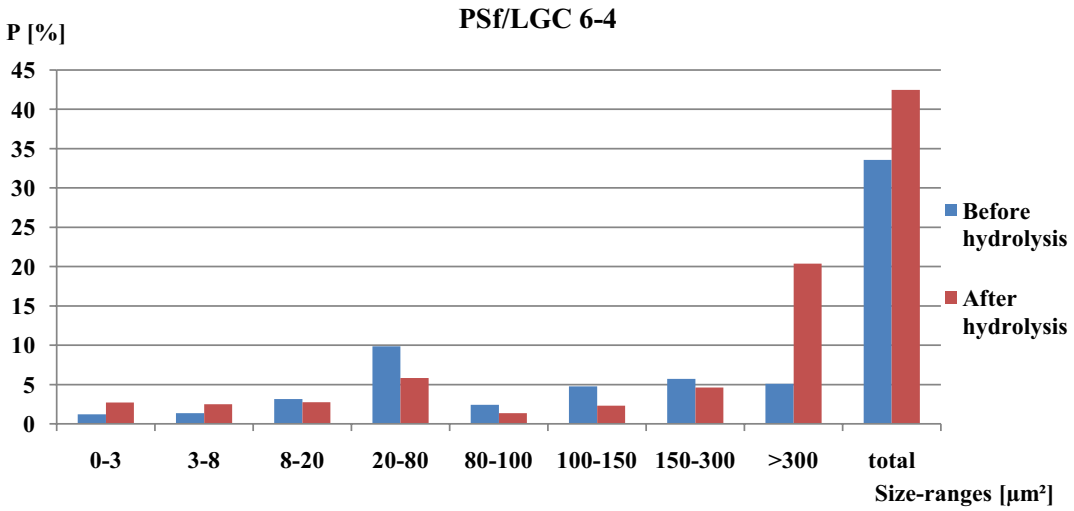

Fig. 8. Differences of porosity *P* [%] for PSf/LGC 6–4 membrane before and after hydrolysis (for eight area ranges in relation to the whole area membrane).

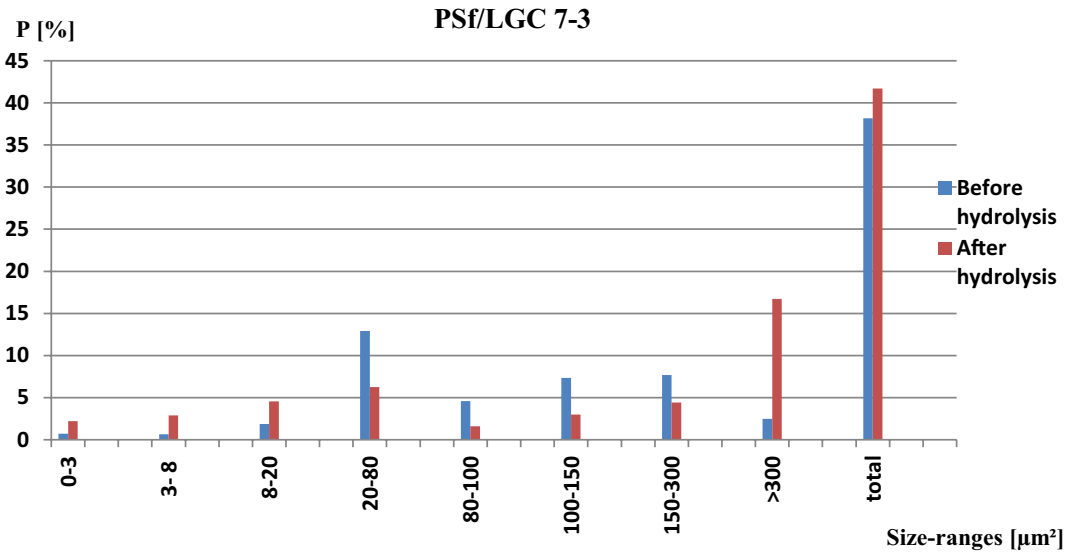

Fig. 9. Differences of porosity *P* [%] for PSf-LGC 7–3 membrane before and after hydrolysis (for eight area ranges in relation to the whole area membrane).

over half of the LGC removal from the membranes (from 55 to 75 wt.%).

The FTIR analysis carried out for the Psf/LGC 7/3 membrane gives the expected evidence of disappearance of ester groups from the LGC polymer after the hydrolysis process, which proves its degradation and leaching from the membrane structure.

The SEM measurements confirmed the creation of more porous structure after hydrolysis. It was observed that the coefficients of hydraulic permeability (UFC) increased significantly from 2.8 to 10.7 times for all types of membranes after the hydrolysis.

The separation properties of membranes did not significantly change after hydrolysis due to retaining unchanged membranes' MWCO. The change in membrane's selectivity was not significant.

A computer analysis of membrane SEM images carried out using MeMoExplorer revealed significant changes in the structure of pores after hydrolysis, where the number of pores with the largest size of more than 300 µm increased four times after hydrolysis. The overall porosity of membranes has also increased.

The amount of LGC eluted from the membranes is in the range of 55%–75% and does not depend on its content in the membrane. There is no clear upward or downward trend. UFC, on the other hand, increases with increasing LGC content in the membrane both before and after hydrolysis. The values of retention coefficients are similar for all

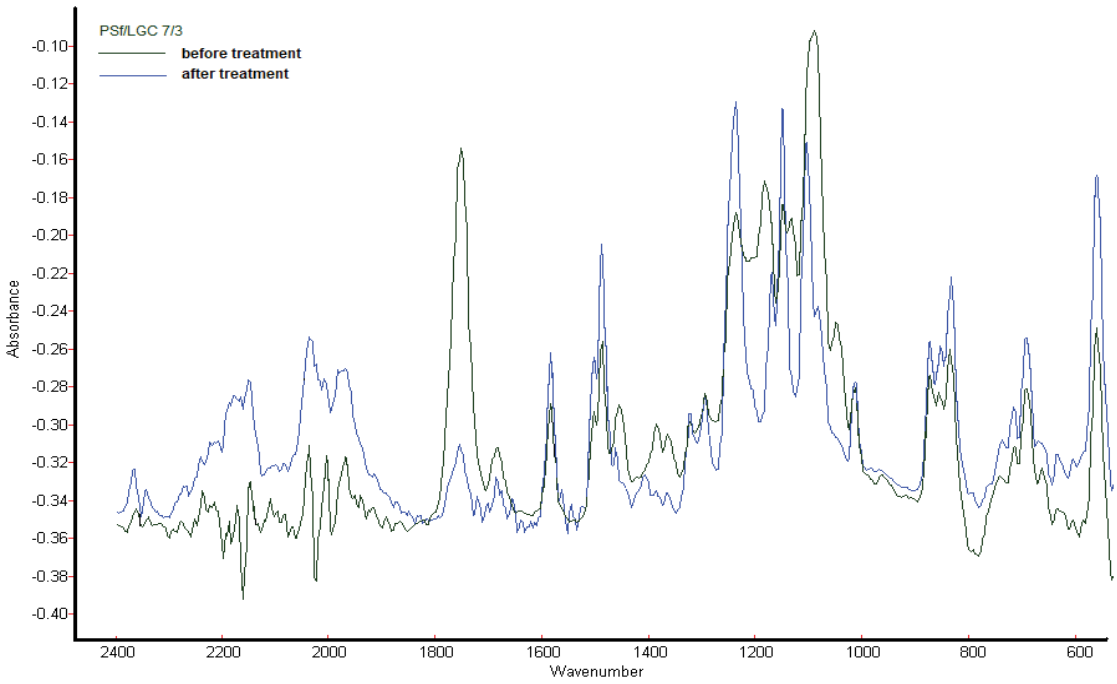

Fig. 10. Reflection spectrum of PSf/LGC 7/3 membrane before hydrolysis (in green) and after hydrolysis (in blue).

membranes and do not depend on the amount of LGC in the membrane. When comparing the porosity of two membranes with an LGC content of 30% and 40%, respectively, we do not notice a significant difference. In summary, the increase in LGC content in the membrane only affects UFC.

The LGC polymer was applied as a classic, degradable porophore for the increase membrane porosity. Porosity changes in structure caused increased membrane permeability. The PSf/LGC membrane after partial removal of LGC exhibited higher porosity, lower retention and higher membrane flux efficiency than the initial PSf/LGC membranes.

In an aqueous environment in which we usually use capillary membranes, the applied by us slow-decomposing LGC polymer (in a two-component PSF/LGC membrane) will be slowly removed from the structure during the operation of the membranes. Progressive partial degradation of the membrane causes the expansion of the existing and formation of the new pores, resulting in a looser membrane structure. Simultaneously, progressive fouling of the membranes will cause the pores clogging and will hinder the medium flow through the membrane. These two opposed processes create a certain balance of media flow efficiency. In this way, the fouling is largely reduced, allowing for a longer working life of the membranes without compromising the efficiency of the membrane processes. In this way, we obtain significant economic benefits, especially in biotechnology, when it is difficult or impossible to regenerate or replace membranes during operation.

References

[1] J. Ren, B. O'Grady, G. de Jesus, J.R. McCutcheon, Sulfonated polysulfone supported high performance thin film composite membranes for forward osmosis, Polymer, 103 (2016) 486–497.

[2] I. Cabasso, C.N. Tran, Polysulfone hollow fibres. II. Morphology, J. Appl. Polym. Sci., 23 (1979) 2967.

[3] S.-H. Chen, R.-M. Liou, Y.-Y. Liu, C.L. Lai, J.-Y. Lai, Preparation and characterizations of asymmetric sulfonated polysulfone membranes by wet phase inversion method, Eur. Polym. J., 45 (2009) 1293–1301.

[4] K. Rodemann, E. Staude, Synthesis and characterization of affinity membranes made from polysulfone, J. Membr. Sci., 88 (1994) 271–278.

[5] P. Aptel, N. Abidine, F. Ivaldi, J.P. Lafaille, Polysulfone hollow fibers ± effect of spinning conditions on ultrafiltration properties, J. Membr. Sci., 22 (1985) 199–215.

[6] H. Ohya, S. Shiki, H. Kawakami, Fabrication study of polysulfone hollow-fiber microfiltration membranes: optimal dope viscosity for nucleation and growth, J. Membr. Sci., 326 (2009) 293–302.

[7] D.S. Kim, J.S. Kang, Y.M. Lee, The influence of membrane surface properties on fouling in a membrane bioreactor for wastewater treatment, Sep. Sci. Technol., 39 (2005) 833–854.

[8] P.S. Goh, W.J. Lau, M.H.D. Othman, A.F. Ismail. Membrane fouling in desalination and its mitigation strategies, Desalination, 425 (2018) 130–155.

[9] A.L. Lewis, Phosphorylcholine-based polymers and their use in the prevention of biofouling, Colloids Surf., B, 18 (2000) 261–275.

[10] N. Hilal, O.O. Ogunbiyi, N.J. Miles, R. Nigmatullin, Methods employed for control of fouling in MF and UF membranes: a comprehensive review, Sep. Sci. Technol., 40 (2005) 1957–2005.

[11] Y.Q. Wang, T. Wang, Y.L. Su, F. Peng, H. Wu, Z.Y. Jiang, Remarkable reduction of irreversible fouling and improvement of the permeation properties of poly(ethersulfone) ultrafiltration membranes by blending with Pluronic F127, Langmuir, 21 (2005) 11856–11862.

[12] Y.Q. Wang, Y.L. Su, X.L. Ma, Q. Sun, Z.Y. Jiang, Pluronic polymers and poly-ethersulfone blend membranes with improved fouling resistant ability and ultrafiltration performance, J. Membr. Sci., 283 (2006) 440–447.

[13] A. Ul Haq Khan, Z. Khan, I.H. Aljundi, Improved hydrophilicity and anti-fouling properties of polyamide TFN membrane comprising carbide derived carbon, Desalination, 420 (2017) 125–135.

[14] W. Li, X. Su, A. Palazzolo, S. Ahmed, E. Thomas, Reverse osmosis membrane, seawater desalination with vibration assisted reduced inorganic fouling, Desalination, 417 (2017) 102–114.
[15] K. Kim, P. Sun, V. Chen, D.E. Wiley, A.G. Fane, The cleaning of ultrafiltration membranes fouled by protein, J. Membr. Sci., 80 (1993) 241–249.
[16] J. Diep, A. Tek, L. Thompson, J. Frommer, Y.H. La, Layer-by layer assembled core-shell star block copolymers for fouling resistant water purification membranes, Polymer, 103 (2016) 468–477.
[17] M. You, P. Wang, M. Xu, T. Yuan, J. Meng, Fouling resistance and cleaning efficiency of stimuli-responsive reverse osmosis (RO) membranes, Polymer, 103 (2016) 457–467.
[18] H. Therien-Aubin, L. Chen, C.K. Ober, Fouling-resistant polymer brush coatings, Polymer, 52 (2011) 5419–5425.
[19] D.J. Miller, D.R. Paul, B.D. Freeman, An improved method for surface modification of porous water purification membranes, Polymer, 55 (2014) 1375–1383.
[20] J.H. Jhveri, Z.V.P. Murthy, A comprehensive review on anti-fouling nanocomposite membranes for pressure driven membrane separation processes, Desalination, 379 (2016) 137–154.
[21] M. Padaki, D. Emadzadeh, T. Masturra, A.F. Ismail, Antifouling properties of novel PSf and TNT composite membrane and study of effect of the flow direction on membrane washing, Desalination, 362 (2015) 141–150.
[22] X. Zhang, B. Lin, K. Zhao, J. Wei, J. Li, A free-standing calcium alginate/polyacrylamide hydrogel nanofiltration membrane with high anti-fouling performance: preparation and characterization, Desalination, 362 (2015) 234–241.
[23] J. Kim, D. Suh, C. Kim, Y. Baek, B. Lee, H. Joong Kim, J. Lee, J. Yoon, A high-performance and fouling resistant thin-film composite membrane prepared via coating TiO_2 nanoparticles by sol-gel-derived spray method for PRO applications, Desalination, 397 (2016) 157–164.
[24] P. Czekaj, W. Mores, R.H. Davis, C. Güell, Infrasonic pulsing for foulant removal in crossflow microfiltration, J. Membr. Sci., 180 (2000) 157–169.
[25] K.D. Miller, S. Weitzel, V.G.J. Rodgers, Reduction of membrane fouling in the presence of high polarization resistance, J. Membr. Sci., 76 (1993) 77–83.
[26] P. Aerts, I. Genne, S. Kuypers, R. Leysen, I.F.J. Vankelecom, P.A. Jacobs, Polysulfone-aerosil composite membranes: Part 2. The influence of the addition of aerosil on the skin characteristics and membrane properties, J. Membr. Sci., 178 (2000) 1–11.
[27] S.H. Yoo, Y.H. Kim, Y.H. Yho, J. Won, Y.S. Kang, Influence of the addition of PVP on the morphology of asymmetric polyimide phase inversion membranes: effect of PVP molecular weight, J. Membr. Sci., 236 (2004) 203–207.
[28] B. Chakrabarty, A.K. Ghoshal, M.K. Purkait, Preparation, characterization and performance studies of polysulfone membranes using PVP as an additive, J. Membr. Sci., 315 (2008) 36–47.
[29] C. Wojciechowski, A. Chwojnowski, L. Granicka, E. Łukowska, M. Grzeczkowicz, Polysulfone/polyurethane blend degradable hollow fiber membranes preparation and transport-separation properties evaluation, Desal. Water Treat., 57 (2016) 22191–22199.
[30] C. Wojciechowski, A. Chwojnowski, L. Granicka, E. Łukowska, Polysulfone/cellulose acetate blend semi degradable capillary membranes preparation and characterization, Desal. Water Treat., 64 (2017) 365–371.
[31] R. Mahendran, R. Malaisamy, D.R. Mohan, Cellulose acetate and polyethersulfone blend ultrafiltration membranes. Part I: preparation and characterizations, Polym. Adv. Technol., 15 (2004) 149–157.
[32] E. Pamula, E. Menaszek, *In vitro* and *in vivo* degradation of poly(L-lactide-co-glycolide) films and scaffolds, J. Mater. Sci. – Mater. Med., 19 (2008) 2063–2070.
[33] P. Dobrzynski, Synthesis of biodegradable copolymers with low-toxicity zirconium compounds. III. synthesis and chain-microstructure analysis of terpolymer obtained from L-lactide, glycolide, and ε-caprolactone initiated by zirconium(IV) acetylacetonate, J. Polym. Sci., Part A: Polym. Chem., 40 (2002) 3129–3143.
[34] M. Przytulska, A. Kruk, J.L. Kulikowski, C. Wojciechowski, A. Gadomska-Gajadhur, A. Chwojnowski, Comparative assessment of polyvinylopyrrolidone type of membranes based on porosity analysis, Desal. Water Treat., 75 (2017) 18–25.